

Figure 1 Sea-surface distribution of suspended sulphur granules. Quasi-true-colour images for the region at latitude 12° E–16° E, longitude 22° S–27° S, off south-central Namibia; images were generated from the OrbView-2 SeaWiFS satellite during March–April 2001. The milky turquoise coloration represents high concentrations of suspended sulphur granules. Data were collected on **a**, 18 March; **b**, 29 March; and **c**, 3 April 2001.

reflective precipitated microgranules of sulphur resulting from the oxidation of sulphide ions near the oxygenated sea surface.

In the days that followed, the feature was observed from satellite pictures to be advected northwards and offshore in the prevailing equatorward geostrophic current flow and offshore-directed surface-wind drift fields, which are characteristic of such eastern-ocean coastal upwelling systems⁴, to reach the position and configuration seen in Fig. 1b. In the image of 3 April (Fig. 1c), even while the earlier offshore feature continues to maintain a coherent identity, another totally new hydrogen sulphide emission event is seen to have started abruptly within the coastal upwelling zone north of Lüderitz.

Once the earlier feature had separated from the coast, it took on an appearance superficially similar to that in satellite views of very large coccolithophore blooms⁵. However, the continuity of the feature in the available satellite views and the advective context, as inferred from the evolution of satellite-sensed ocean surface temperature, make it clear that the offshore feature is the same as that previously observed as an intense episode of sulphide emission nearer the coast. The zone of intense coloration in later images (Fig. 1b) extends over an expanse of total sea surface greater than 20,000 km².

Such episodes have been recorded somewhere along the coast of Namibia more often than not during the recent months since the satellite observational capability was recognized. Where verification on the ground has been available, the early stages of these events have likewise been confirmed to be associated with sulphide emissions. In addition to its directly toxic effects, hydrogen sulphide strips dissolved oxygen from the water column, leaving behind a subsurface hypoxia that is manifested visibly as the sulphur-infused sea surface. It is this subsurface hypoxia,

which might endure well beyond the period when the toxic sulphide gas is present, that could pose the principal ecological problem. An event, first clearly noted on 17 May 2001, was still plainly visible as late as 6 June 2001.

Scarla J. Weeks*, **Bronwen Currie†**, **Andrew Bakun‡**

**Ocean Space Ltd, and †IRD, IDYLE Project, Oceanography Department, University of Cape Town, Rondebosch 7701, South Africa*
e-mail: oceanspace@icon.co.za

‡*National Marine Research and Information Center, Swakopmund, Namibia*

1. Bailey, G. W., Beyers, C. J. deB. & Lipschitz, S. R. *S. Afr. J. Mar. Sci.* **3**, 197–214 (1985).
2. Mas-Riera, J., Lombarte, A., Gordo, A. & Macpherson, E. *Marine Biol.* **104**, 175–182 (1990).
3. Hamukuaya, H., O’Toole, M. J. & Woodhead, P. M. J. *S. Afr. J. Mar. Sci.* **19**, 57–59 (1998).
4. Wooster, W. S. & Reid, J. L. in *The Sea Vol. 2* (ed. Hill, M. N.) 253–280 (Interscience, New York, 1963).
5. Tyrrell, T., Holligan, P. M. & Mobley, C. D. *J. Geophys. Res.* **104**, 3223–3241 (1999).

Competing financial interests: declared none.

Biomechanics

Dinosaur locomotion from a new trackway

Ardley Quarry in Oxfordshire, UK, contains one of the most extensive dinosaur-trackway sites in the world, with individual trackways extending for up to 180 metres. We have discovered a unique dual-gauge trackway from a bipedal theropod dinosaur from the Middle Jurassic in this locality, which indicates that these large theropods were able to run and that they used different hindlimb postures for walking and running. Our findings have implications for the biomechanics and evolution of theropod locomotion.

The Ardley trackways are preserved on a single horizon of the Middle Bathonian

(163 million years old)¹ white-limestone formation and include those from large theropods and at least two types of sauropod dinosaur. Three of the trackways (numbered 13, 29 and 80; J.J.D., unpublished observations) comprise large tridactyl (‘three-toed’) prints, with narrow claw impressions typical of theropod dinosaurs (Fig. 1). All three trackways (except for a section of track 13) are wide-gauge, with the prints indicating that the hind feet were placed sequentially in a zig-zag arrangement separated widely from the midline (Fig. 1a). Stride length (2.70 m) and pace angulation (117°–132°; Fig. 1) remain constant throughout the wide-gauge tracks. This pattern contrasts strongly with the more usual narrow-gauge form of theropod trackway^{2,3} in which pace-angulation values range between 160° and 170°: the hind-foot impressions are located close to the midline of the trackway.

Trackway 13 is unique because one section shows the theropod gait switching from wide to narrow gauge (the stride length increases to 5.65 m and pace angulation increases to 173°; Fig. 2). The orientation of the feet also changes from positive rotation (toes directed forwards and inwards; Fig. 1a) during wide-gauge locomotion, to a small negative rotation (toes directed slightly outwards) during the narrow-gauge phase (Fig. 1b).

Estimating the speed of movement of the track-maker requires information on

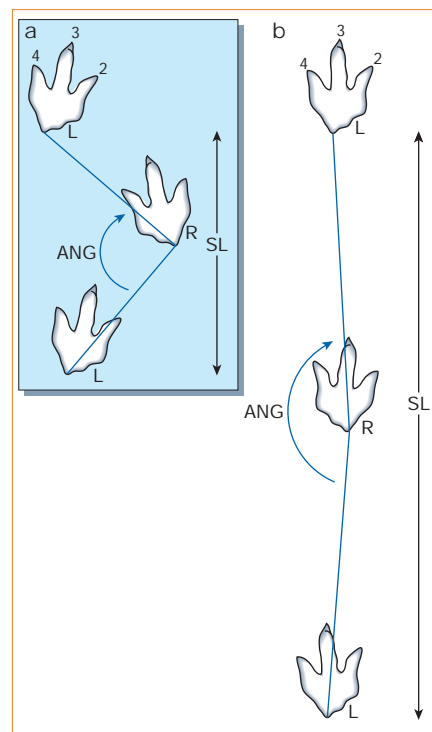


Figure 1 The dual-gait features of theropod trackway 13 from Ardley Quarry, Oxfordshire, UK. **a**, Wide-gauge section; **b**, narrow-gauge section. Digits are numbered and footprints are identified as left (L) and right (R); ANG, pace angulation; SL, stride length.

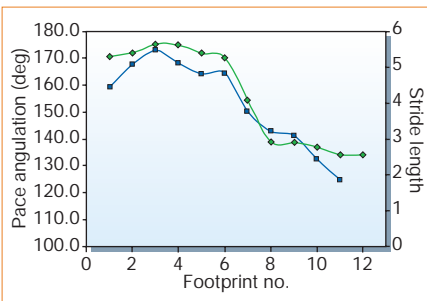


Figure 2 Deceleration phase of the ‘running’ section of trackway 13. Blue, pace angulation; green, stride length. Prints preceding this section are missing but global-positioning satellite data (J.J.D., unpublished observations) indicate that this section is continuous with the rest of trackway 13.

hip height (h) and stride length^{3,4}. Hip height can be calculated from foot length³ (which equals the length of the middle toe, ‘digit III’). For trackway 13, this gives an h value of 1.93 m, giving estimated speeds of 6.8 km h⁻¹ and 29.2 km h⁻¹ for the wide- and narrow-gauge segments, respectively.

Placing the hind feet close to, or on, the midline⁵, optimizes locomotor efficiency by maximizing the effective stride length and reducing the energy lost through lateral displacement of the centre of gravity. The Ardley trackways therefore have important implications for the locomotor styles of large theropod dinosaurs. The simultaneous alteration of stride length and pace angulation (Fig. 2), foot orientation and estimated speeds all suggest that the large Ardley theropod used the wide-gauge gait while walking but was capable of a ‘gear change’ to maximize running ability by employing the more efficient, narrow-gauge gait.

Greater stability was probably achieved during walking by shortening the stride length, placing the hind feet further from the midline and rotating the feet inwards. Although providing more stability, the wider spacing of the hindlimbs would decrease the maximum stride length and therefore the attainable speed, so faster locomotion would have called for a change to the narrow-gauge gait.

Trackway evidence of the running ability of large bipedal dinosaurs is scant⁶. Estimates of maximum speeds obtained from biomechanical studies of skeletal material are controversial, particularly for large theropods³. The increase in stride length evident in trackway 13 indicates that at least some large theropods were capable of running at speeds close to previous maximum estimates.

Other issues concerning locomotion in large theropods remain to be resolved. The narrow-gauge (running) section of trackway 13 is only 35 m long and leaves unanswered the question of how long a large theropod could sustain a running gait. It is also uncertain whether the wide-gauge gait

was habitually adopted by large theropods while walking, or only when the ground was very soft or unstable. Furthermore, the anatomical correlations between leg and hip anatomy associated with the adoption of wide- and narrow-gauge gaits are not yet known and we are therefore unable to determine the phylogenetic distribution of these locomotor styles. Nevertheless, the Ardley trackways offer new insight into dinosaur locomotor capacity and will stimulate enquiry into the evolution and biomechanics of large theropod dinosaurs.

Julia J. Day*, **David B. Norman***, **Paul Upchurch***, **H. Philip Powell†**

*Department of Earth Sciences, University of Cambridge, Downing Street, Cambridge CB2 3EQ, UK

e-mail: jday00@esc.cam.ac.uk

†Oxford University Museum of Natural History, Parks Road, Oxford OXD1 3PW, UK

1. Cope, J. C. W. *et al. Geol. Soc. Spec. Rep.* **15** (1980).
2. Padian, K. & Olsen, P. E. *Copeia* **1984**, 662–671 (1984).
3. Thulborn, R. A. *Dinosaur Tracks* (Chapman & Hall, London, 1990).
4. Alexander, R. M. *Nature* **261**, 129–130 (1986).
5. Alexander, R. M. *Zool. J. Linn. Soc.* **83**, 1–25 (1986).
6. Thulborn, R. A. *Nature* **292**, 273–274 (1981).

Fish physiology

Dogfish hair cells sense hydrostatic pressure

Many marine invertebrates and fish respond to hydrostatic pressure in order to regulate their depth and synchronize their behaviour to tidal cycles^{1–4}. Here we investigate the effect of hydrostatic pressure on the vestibular hair cells located in the labyrinth of the dogfish *Scyliorhinus canicula*, and find that it modulates their spontaneous activity and response to angular acceleration. This may explain not only the low resting activity of vertebrate hair cells but also how fish that do not have swim bladders can sense hydrostatic cues.

How a hydrostatic-pressure-sensing mechanism could exist in animals that have no gas compartment remained a mystery⁵ until the discovery of a piston mechanism in crabs⁶, in which differential compression of the outer cuticle and the internal fluid of thread hairs in the balancing system leads to nanometre-level displacements that are sensed by mechanoreceptors⁶. Cells in culture may respond to tiny changes in hydrostatic pressure¹ by altering their division or in other ways, although isolated cochlear hair cells show no significant length or transmembrane-voltage changes in response to increased hydrostatic pressure⁷.

We made extracellular recordings from

vestibular type-II hair cells in horizontal canal units in isolated elasmobranch labyrinths, a well-known model system⁸, from seven dogfish to test the sensitivity of these cells to hydrostatic pressure. Nerve spikes were conventionally amplified, filtered and recorded. A computer-controlled pressure regulator produced a test sequence of 1 hour at atmospheric pressure (taken as zero bar) followed by 1 hour at 14 kilopascals (kPa; 0.14 bar) and four sinusoidal pressure cycles of a further 30-kPa amplitude and 15-min period. To stimulate the vestibular system, the preparation was mounted on an Inland DC Servomotor system inside a pressure chamber. A bout of 64 cycles of oscillation around the vertical axis at 1 Hz and 70 deg amplitude was supplied every 2 min. Single units (sets of nerve-spike activity from single neurons) or small groups of units were averaged online or counted offline. Temperature changes were restricted to less than 0.5 °C per hour.

Units responded unidirectionally to oscillation at 1 Hz. Resting and oscillation-derived spike densities (Fig. 1) increased significantly (Mann–Whitney U -test) after the pressure step. During, but not preceding, the imposed hydrostatic-pressure cycles, related cyclical changes in spike frequency were confirmed by using autocorrelation and maximum-entropy spectral analysis⁹. There was a positive relationship between spike frequency and hydrostatic pressure but not between spike frequency and rate of pressure change.

The changes in resting and angular-acceleration-derived activity after a change in hydrostatic pressure could be part of a depth-sensing mechanism in fish and may explain the signalling value of low resting activity in hair cells. It is likely that differential compression leads to nanometre-scale strains that activate the hair cells directly.

This finding has implications for transduction mechanisms in a variety of hair-cell types, including cochlear hair cells, in

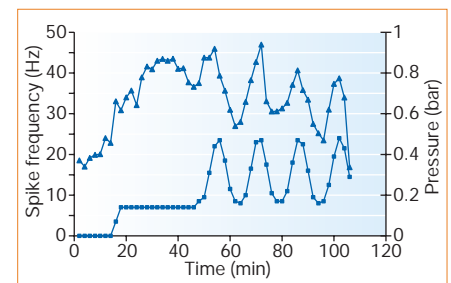


Figure 1 Average extracellular spike frequencies from a small set of units from the dogfish right vestibular system during bouts of 64 oscillation cycles (top trace) and hydrostatic pressure (bottom trace) recorded every 2 min. Oscillation-derived activity increases significantly after the change in pressure and shows cyclical changes with the same 15-min period as the imposed pressure cycles.